

The Discrepancy in Timing Between Synchronous Signals and Visual Stimulation Should not be Underestimated

Biao CHEN¹, Xu JIANG², Ping WANG³, Zhuoyun WANG¹, Shengzhao ZHANG^{2*}, Zhen LIANG^{2*}

¹ (Second Affiliated Hospital of Anhui Medical University, Anhui Hefei 230601, China)

² (School of Biomedical Engineering, Anhui Medical University, Anhui Hefei 230032, China)

³ (School of Innovation and Entrepreneurship, Anhui Medical University, Anhui Hefei 230032, China)

[Abstract] Response latency (RT) is a critical parameter in studying human behavior, representing the time interval between the onset of a stimulus and the subject's response. However, different time base between devices can introduce errors in RT measurements. Serial port synchronization signal can mitigate this error, but limited information is available regarding their accuracy. Optical signals offer another option, but the difference in the positioning of optical signals and visual stimuli can introduce errors, and there have been no reported to reduce this. This study aims to investigate methods for reducing the time errors. We used the PsychToolbox to generate visual stimuli and serial port synchronization signals to explore their accuracy. Subsequently, we propose and validate a calibration formula to minimize the error between optical signals and visual stimuli. The findings as follows: Firstly, the serial port synchronization signal presenting precedes visual stimulation, with a smaller lead time observed at higher refresh rates. Secondly, the lead time increases as the stimulus position deviates to the right and downwards. Additionally, in Linux and IOPort(), serial port synchronization signals exhibited greater accuracy. Considering the poor timing accuracy and the multiple influencing factors associated with serial port synchronization signals, it is recommended to employ optical signal measuring the RT. The validation results indicate that under the darkening process, the time error is $-0.23 \pm 0.06 \sim -0.01 \pm 0.07$ ms (MEAN \pm SD). This calibration formula can use optical signals to help measure RT accurately. This study provide valuable insights for optimizing experimental design and improving the accuracy of RT measurements.

[Key words] Reaction latency; Synchronous signal; Correction function; Visual stimulation; Timing

² Fund Projects: the Social Science Foundation of Anhui Province of China under Grant (No. AHSKF2019D014)

* Corresponding Author:

1. Zhen Liang, Doctoral, Associate Professor, Anhui Hefei, zliang@ahmu.edu.cn

2. Shengzhao Zhang, Doctoral, Anhui Hefei, zsz1990@ahmu.edu.cn

Introduction

Response latency refers to the time delay between the onset of a stimulus and the initiation of a response (Levakova, Tamborrino, Ditlevsen, & Lansky, 2015), which provides valuable information for understanding temporal coding. Response latency has been widely studied across various cognition research tasks, including simple visual and auditory detection tasks, as well as more complex tasks such as lexical decision tasks (Arieh & Marks, 2008; Eileen L. Troconis et al., 2016; Yap, Balota, Cortese, & Watson, 2006).

Accurate measurements of response latency require recording of the onset time of a stimulus or task and the time of a subject's response, with millisecond accuracy. Achieving this measurement involves the collaboration of multiple devices, it would be ideal that all devices are represented in the same time base (Nguyen, Liang, Muggleton, Huang, & Juan, 2019; Zamarashkina, Popovkina, & Pasupathy, 2020). However, different devices often have varying time bases, leading to increased errors. To mitigate this errors, one approach is the time synchronization. After presenting stimuli, the host sends serial port synchronization signals to other devices. However, research by He Feng indicates that the serial port lag ranges from 0.3 ms to 10 ms when transmitting levels, depending on factors such as input pulse frequency, priority, and real-time performance (Feng, Yong, YaBo, & Rui, 2009). The delay can be even worse when transmitting multi-characters. While He Feng's work did not involve the psychology-specific tools, it still underscores the importance of accurately synchronizing signal transmission times. Li Xiangrui converted the time of the response collection device (Rtbox) into the time of the stimulus generating device, compensating for the transmission time of the synchronous signal (Xiangrui, Liang, Kleiner, & Zhong-Lin, 2010). Although this approach is particularly useful when using devices that lack built-in time synchronization capabilities, such as keyboards and mice, it does increase the experimental complexity. The optimal solution lies in configuring the corresponding parameters on the PC to clarify and reduce synchronization signal transmission times, reducing errors in response latency measurements.

Optical signals, serving as external trigger signals, offer another viable option for measuring response latency accurately. In this approach, an external measuring device, triggered by the optical signal displayed on the monitor, can precisely record the timestamp corresponding to the presentation of the optical signal as the timestamp for visual stimulation. (Xiangrui et al., 2010). This method does not require time synchronization since the stimulus and response operate on the same time base. However, it is essential to

acknowledge that an inherent error exists between the optical signal and the visual stimuli due to disparities in their respective positions. This discrepancy arises because LCD monitors conform to the same raster scan mechanism as CRTs (T & L, 2010). The maximum theoretical error, assuming a refresh rate of 60 Hz and a resolution of 1920 * 1080, can be up to 16.67ms. There is no effective method have been proposed to reduce the error. Further research is needed to explore potential solutions for minimizing the error between optical signals and visual stimuli.

This study has the primary objective of investigating methods to reduce synchronization signal and visual stimulus errors in order to achieve accurate response latency measurements. The study consists of three experiments: Experiment I, Experiment II and Experiment III. Experiment I focuses on exploring the timing and error associated with serial port synchronization signals and visual stimuli. The aim is to identify potential sources of error and develop strategies to optimize accuracy. Due to the instability of the serial port signal cycle, there is significant jitter in the time error. In order to stabilize the serial port signal cycle, we conducted Experiment II. Experiment II mainly studies the influencing factors of the serial port signal cycle, aiming to improve the stability of it. Experiment III introduces a calibration formula, which aims to studies methods for reducing the errors between optical signals and visual stimuli. This calibration formula leverages the optical signal to precisely calculate the presentation time of visual stimuli to obtain more accurate response latency. The study aims to contribute to the field by providing insights into reducing errors in synchronization signals and visual stimuli, ultimately enhancing the accuracy of response latency measurements.

Materials and methods

In this study, a phototransistor (EVERLIGHT, PT908-7C-F) was attached to an computer's monitor to detected changes of the light on the screen (Fig. 1). Once the optical signal was converted into an electrical signal through photoelectrical conversion, it was transmitted to a logic analyzer (Saleae logic pro 8, USA). USB interfaces have gained popularity as the preferred choice for PC connections due to their support for hot swapping and easy expandability. However, the serial port data transmission protocol is well supported by all the commonly used operating systems and most experimental toolkits. To ensure compatibility with both interface types, we adopted a simple and popular solution by implementing a standard serial bus protocol on top of the USB protocol by use of a USB-to-serial converter chip. The sampling rate of the logic

analyzer was set to 6.25 MS/sec for digital signals and 781.25 KS/sec for analog signals. It is worth noting that the API function used during the test was IOPort() and the operation system is Windows unless otherwise specified.

Computers

The system, as depicted in Figure 1, consisted of two computers: Computer 1 and Computer 2. Computer 1, referred to as the tested device, was a desktop computer running Windows 10 64-bit Professional Edition. It was equipped with an Intel i7-4790 core processor and an AMD Radeon R7 200 Series GPU. The display used in Computer 1 was a PHILIPS 322M7C LCD monitor with a 1ms response time and a resolution of 1920 * 1080 pixels. This computer served as the main device responsible for generating visual stimuli. Computer 2, referred to as the data processing device, played a role in receiving and processing the data transmitted by the logic analyzer. It was specifically dedicated to handling the captured data and performing subsequent analysis and processing tasks.

Stimuli and synchronization signal

PsychToolbox was utilized to generate both the visual stimuli and the serial port synchronization signals in this study. The visual stimuli consisted of a black block and a white block, while the remaining parts of the monitor were set to gray. Each block had dimensions of 300×300 pixels and alternated at a frequency of 10 Hz. Immediately following the presentation of the black block, the decimal number 170 was sent from the test device to the logic analyzer through serial port. Similarly, after the white block, the decimal number 85 was sent through serial port. This process was repeated for a total of 10,000 cycles. The serial baud rate used for transmission was set at 9600 bits per second, and the experimental process was executed at the highest priority level. To minimize variation due to the temperature dependence of the LCD monitor's response time (H & A, 2007; Zhang et al., 2018), all measurements were taken after the monitor had been turned on for a minimum of 60 minutes, allowing for a sufficient warm-up period.

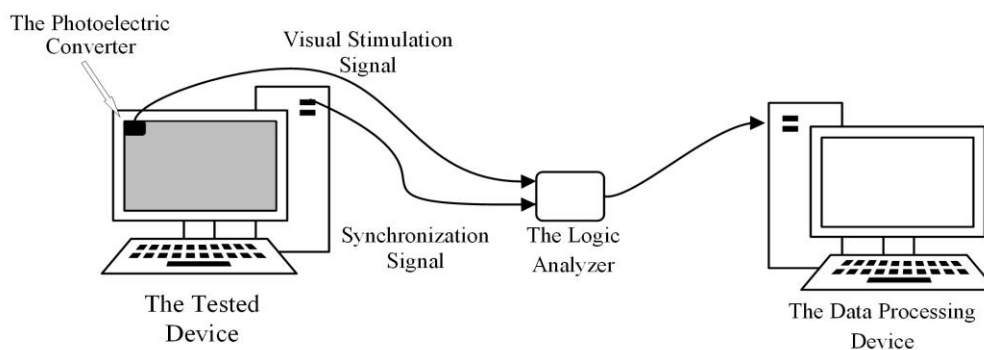


Fig.1 Experimental Setup for Timing and Error Measurements. Visual stimuli were converted into electrical signals by a photoelectric converter. A logic analyzer collected photoelectric converter signal and serial port synchronous signal at the same time.

Data analysis

In the context of LCD monitors, the response time can vary unevenly when transitioning between different grayscale levels (H & A, 2007; T, 2010; T & G, 2009; T & L, 2010). This results in distinct processes for the rising and falling edges of the visual stimulus waveforms. To simplify terminology and clarify these processes, the rising edge (transition from a white block to a black block) is referred to as the "darkening process," while the falling edge (transition from a black block to a white block) is called the "brightening process." Fig. 2 illustrates a waveform captured during the experiment. The upper part of the waveform represents the serial synchronization signal, while the lower part represents the visual stimulation signal. To determine the switching point of the visual stimulus, a threshold is defined. In this case, the threshold is set as half of the highest voltage of the visual stimulation signal. The timestamps at which the visual stimulation signal rises or falls to the threshold are denoted as T_1 and T_2 , respectively. Similarly, the timestamp at which the serial synchronization signal first falls to low level is denoted as T_{S1} or T_{S2} . By establishing these definitions and timestamps, researchers can precisely measure the timing and analyze the temporal relationship between the visual stimuli and the serial synchronization signal.

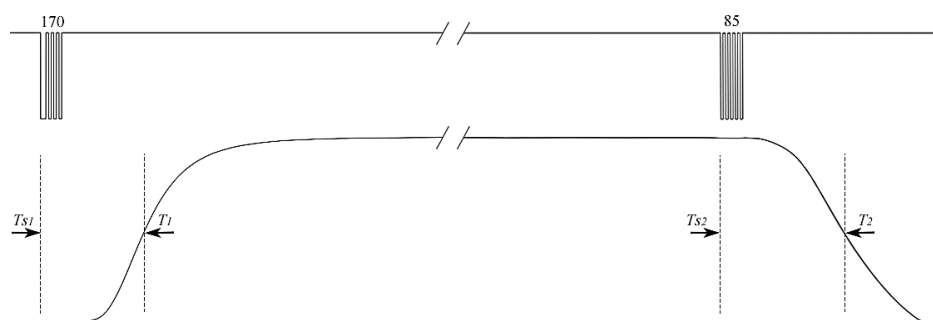


Fig.2 Definition of Timestamps. Threshold for Visual Stimulus Switching: The threshold is set as half of the highest voltage of the visual stimulation signal. It serves as a reference point to determine when the visual stimulus transitions from one state to another. T_1 represents the timestamp when the visual stimulation signal rises to the threshold level, indicating the start of the darkening process. T_2 represents the timestamp when the visual stimulation signal falls to the threshold level, marking the beginning of the brightening process. T_{s1} and T_{s2} : The timestamp for when the serial port synchronization signal first fell to low level.

$$T_a = T_{s1} - T_1 \quad (1)$$

$$T_b = T_{s2} - T_2 \quad (2)$$

The time error of the darkening process (T_a) and the brightening process (T_b) can be calculated using formulas (1) and (2). In these formulas, a negative bias indicates that the serial port synchronization signal leads the visual stimuli, while a positive bias suggests that the visual stimuli lead the serial port synchronization signal. By subtracting the respective timestamps, researchers can determine the time error for each process. Analyzing and interpreting these time errors allows researchers to understand the temporal relationship and potential discrepancies between the serial port synchronization signal and the visual stimuli during the darkening and brightening processes.

Results

Experiment I

We measured the timing of the visual stimuli and serial port synchronization signals, and analyzed the effects of USB to serial adapter, refresh rate, and stimulus presentation position. The USB to serial adapters used in the experiment included CH340G (WCH, China), FT232RL (FTDI, UK), and PL2303HX (PROFIC, China). The refresh rates investigated were 60 Hz, 100 Hz, and 120 Hz. The stimulus presentation positions studied were the upper left corner, center, and bottom right corner of the screen. For each stimulus presentation position, the coordinates of the visual stimulus and the photoelectric converter were recorded. In the upper left corner, the visual stimulus coordinates were [0,0,300,300], and the photoelectric converter coordinates were [140,91,141,92]. In the center, the visual stimulus coordinates were [810,390,1110,690], and the photoelectric converter coordinates were [957,519,958,520]. In the bottom right corner, the visual stimulus coordinates were [1620,780,1920,1080], and the photoelectric converter coordinates were [1761,908,1762,909]. To analyze the data, GraphPad Prism 8 was used to generate frequency distribution maps. These maps represented the occurrence of time errors in the horizontal axis (measured in milliseconds)

and the number of occurrences with a 0.1ms delay on the vertical axis. For ease of visualization, the vertical axis employed logarithmic coordinates with a base of 10.

Figure.3 presents the timing and time error analysis under different USB to serial adapters. The experiment was conducted with a refresh rate of 60Hz, and the stimulus was presented in the upper left corner. Observing the data in Figure 3, it can be observed that both T_a and T_b are negative, indicating that the serial port synchronous signal leads the visual stimulus, contrary to the intended experimental design. Interestingly, no significant difference in time error is observed among the different USB to serial adapters. Figures 3A and 3B, generated using the CH340G adapter, show that $T_a = -4.06 \pm 0.14\text{ms}$ (MAX: -2.98ms, MIN: -4.83ms), and $T_b = -5.44 \pm 0.14\text{ms}$ (MAX: -4.58ms, MIN: -6.22ms). Figures 3C and 3D, produced using the FT232RL adapter, indicate that $T_a = -3.88 \pm 0.13\text{ms}$ (MAX: -2.88ms, MIN: -4.63ms), and $T_b = -5.26 \pm 0.13\text{ms}$ (MAX: -4.15ms, MIN: -6.00ms). Figures 3E and 3F, generated using the PL2303HX adapter, demonstrate that $T_a = -3.99 \pm 0.15\text{ms}$ (MAX: -3.02ms, MIN: -4.73ms), and $T_b = -5.28 \pm 0.15\text{ms}$ (MAX: -4.29ms, MIN: -6.05ms).

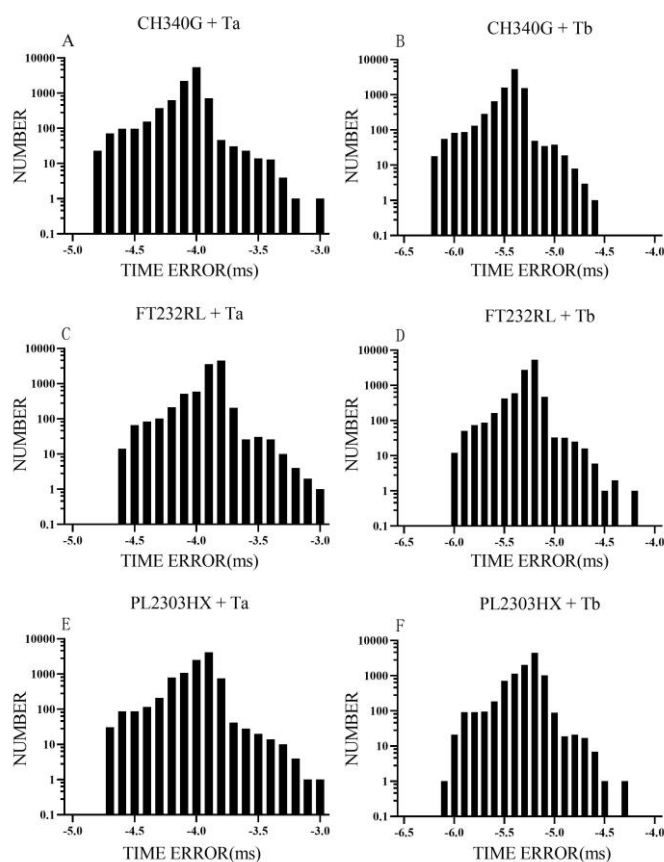


Fig.3 Distributions of Time Error for Different USB to Serial Adapters. Across all three USB to serial adapters (CH340G, FT232RL, and PL2303HX), the distributions of time error consistently exhibit negative values, indicating that the serial port

synchronous signal leads the visual stimulus rather than lags behind it. This observation is contrary to the intended experimental design. The distributions of time error are similar for all three USB to serial adapters, suggesting that there is no significant difference in the time synchronization performance among these adapters. This finding implies that the choice of USB to serial adapter may not have a substantial impact on the observed time error.

The refresh rate determines the speed of displaying one frame may affect the time error. Figure 4 demonstrates the effect of different refresh rates on the time error. In this test, the USB to serial adapter used was CH340G, and the stimulus was presented in the upper left corner. The data in Figure 4 indicates that as the refresh rate increases, the absolute value of the time error decreases. However, there is no significant change in the overall accuracy of the measurements. Figures 4A and 4B, generated at a refresh rate of 60Hz, show that $T_a = -4.06 \pm 0.14\text{ms}$ (MAX: -2.98ms , MIN: -4.83ms), and $T_b = -5.44 \pm 0.14\text{ms}$ (MAX: -4.58ms , MIN: -6.22ms). Figures 4C and 4D, produced at a refresh rate of 100Hz, indicate that $T_a = -3.35 \pm 0.14\text{ms}$ (MAX: -2.41ms , MIN: -4.10ms), and $T_b = -4.30 \pm 0.14\text{ms}$ (MAX: -3.44ms , MIN: -5.09ms). Figures 4E and 4F, generated at a refresh rate of 120Hz, demonstrate that $T_a = -3.12 \pm 0.15\text{ms}$ (MAX: -2.12ms , MIN: -3.85ms), and $T_b = -4.15 \pm 0.15\text{ms}$ (MAX: -3.25ms , MIN: -4.89ms).

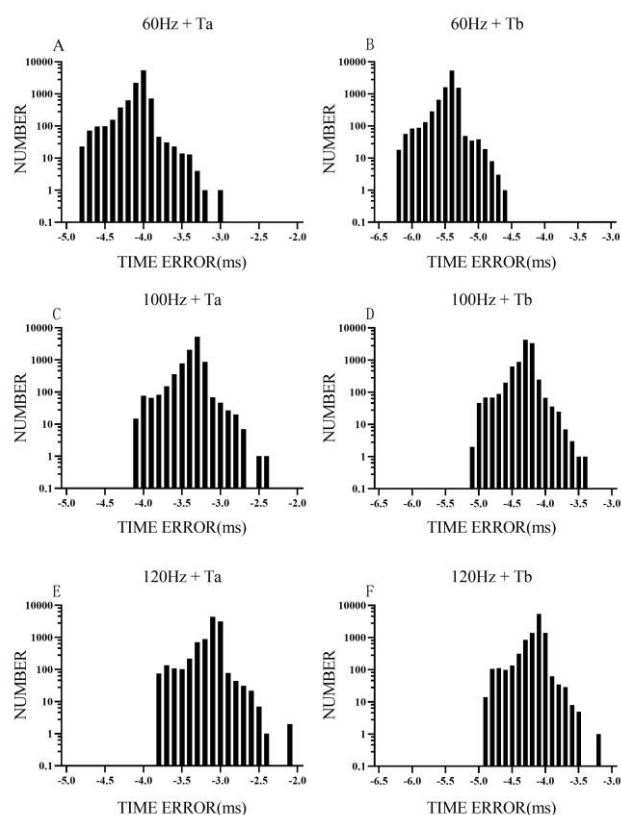


Fig.4 Distributions of Time Error for Different Refresh Rates. The distributions of time error show a shift towards smaller absolute values as the refresh rate increases. A higher refresh rate contributes to improved synchronization between the visual stimuli and the serial port synchronization signal, resulting in reduced time discrepancies.

Since the LCD panels conform to the same raster scan mechanism as CRTs (T & L, 2010), the position may affect the time error. Figure 5 illustrates the effect of different stimulus presentation positions on the time error. The test was conducted using the CH340G USB to serial adapter, with a refresh rate of 60Hz. As observed in Figure 5, when the stimulus presentation position moves from the upper left corner to the bottom right corner, the absolute value of the time error increases. However, there is no significant change in the overall accuracy of the measurements. Figures 5A and 5B, generated for the upper left corner stimulus presentation position, show that $T_a = -4.06 \pm 0.14\text{ms}$ (MAX: -2.98ms , MIN: -4.83ms), and $T_b = -5.44 \pm 0.14\text{ms}$ (MAX: -4.58ms , MIN: -6.22ms). Figures 5C and 5D, produced for the center stimulus presentation position, indicate that $T_a = -10.21 \pm 0.13\text{ms}$ (MAX: -9.29ms , MIN: -11.00ms), and $T_b = -10.95 \pm 0.13\text{ms}$ (MAX: -10.03ms , MIN: -11.68ms). Figures 5E and 5F, generated for the bottom right corner stimulus presentation position, demonstrate that $T_a = -15.83 \pm 0.13\text{ms}$ (MAX: -14.88ms , MIN: -16.59ms), and $T_b = -16.50 \pm 0.13\text{ms}$ (MAX: -15.57ms , MIN: -17.24ms). Researchers should consider the potential impact of stimulus presentation position when designing experiments involving visual stimuli and serial port synchronization signals to minimize time discrepancies and improve synchronization.

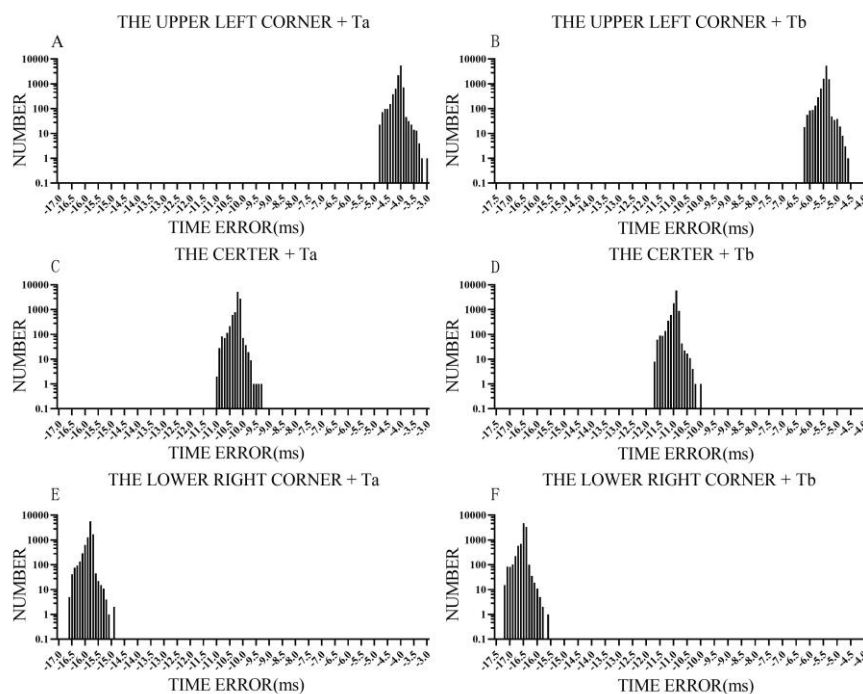


Fig.5 Distributions of Time Error for Different Stimulus Presentation Positions. The distributions of time error clearly demonstrate a shift towards larger absolute values as the stimulus presentation position moves from the top left to the bottom right.

Significant jitter of time error was found in the measurement. To investigate the causation, we separately counted the visual stimulus period and the serial port synchronization signal period. The period data comes from the measurement results of different USB to serial adapters in Experiment I. The timestamp for when the visual stimuli signals first rose to the threshold was defined as the start time of a period and the end of the previous period. The serial port synchronization signal is a series of digital pulses. The timestamp for when the serial port synchronization signal first drops to low level from high level was defined as the start time of a period and the end time of the previous period. Periods were defined as the difference between adjacent timestamps. Table 1 and Table 2 show the visual stimulation period and serial port synchronization signal period during the darkening and brightening processes. We can see that, in the test, the visual stimuli controlled by Psychtoolbox had great accuracy (=100ms for average, < 0.01ms for SD and <= 0.07ms for range) which is similar to the results of other authors (Bridges, Pitiot, R, MacAskill, & W.Peirce, 2020; Gao et al., 2020), better than serial port synchronization signal (=100ms for average, >0.1ms for SD and > 1ms for range). The jitter of the time error may come from the serial port synchronization signal.

Tab.1 Signal period of darkening process (unit: ms). Cells are colored pale green where the periods is "good" (=100ms for average, < 0.01ms for SD and <= 0.07ms for range). A dark pink where the periods is notably "bad" (=100ms for average, >0.1ms for SD and > 1ms for range).

	CH340G1-Ta		FT232RL2-Ta		PL2303HX3-Ta	
	visual	serial port	visual	serial port	visual	serial port
	stimuli	synchronization	stimuli	synchronization	stimuli	synchronization
Average	100.0	100.0	100.0	100.0	100.0	100.0
SD	0.006	0.17	0.006	0.17	0.006	0.17
Range	0.05	1.78	0.05	1.89	0.06	1.89

Tab.2 Signal period of lighting process (unit: ms). Cells are colored pale green where the periods is “good” (=100ms for average, < 0.01ms for SD and <= 0.07ms for range). A dark pink where the periods is notably “bad” (=100ms for average, >0.1ms for SD and > 1ms for range).

	CH340G		FT232RL		PL2303HX	
	visual	serial port	visual	serial port	visual	serial port
	stimuli	synchronization	stimuli	synchronization	stimuli	synchronization
Average	100.0	100.0	100.0	100.0	100.0	100.0
SD	0.008	0.16	0.008	0.16	0.008	0.17
Range	0.07	1.99	0.07	2.01	0.07	2.10

Experiment II

The high-precision synchronization can't be achieved without high-precision visual stimulation signals and high-precision serial port synchronization signals. Therefore, we explored how to improve the accuracy of serial port synchronization signals. Serial port synchronization signals (decimal 170) were generated by Psychtoolbox with the period of 100ms, and collected by a logic analyzer (the sampling rate was 6.25MS/s). Figure 6 illustrates the experimental setup used for accuracy measurements of the serial port synchronization signals. During the test, the refresh rate was set to 60Hz, the serial baud rate was set to 9600bit/s, and the program was given the highest priority to ensure accurate and reliable measurements. GraphPad Prism 8, a statistical analysis and graphing software, was utilized to generate frequency distribution maps of the collected data. The horizontal axis of the frequency distribution maps represents the period of the serial port synchronization signals in milliseconds (ms). To accommodate a wide range of values, the vertical axis adopts logarithmic coordinates with a base of 10.

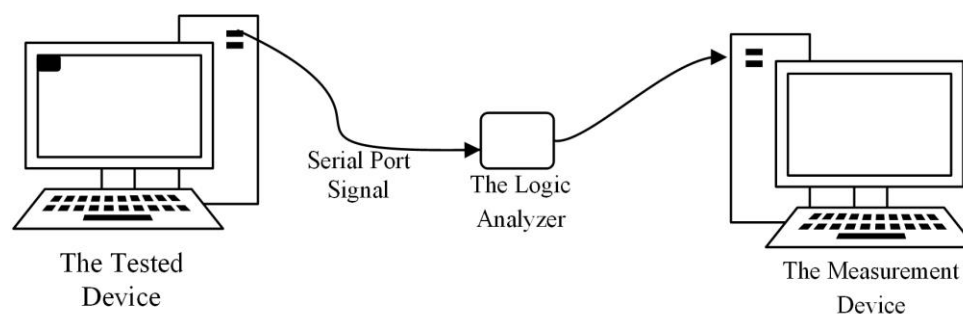


Fig. 6 Experimental Setup of Accuracy Measurements. In this setup, the serial port synchronization signal was generated with a fixed period of 100ms using the Psychtoolbox software. The generated signal was then collected and analyzed using a logic analyzer.

The performance of USB to serial adapters may directly affect the accuracy of serial port synchronization signals. The operating systems may also affect it by different calling mechanisms and complexity. We measured the periodic accuracy of CH340G, FT232RL, and PL2303HX on Windows and Linux. The API function used during the test was IOPort(). Figure 7 displays the comparison of the serial port synchronization signal accuracy for different USB to serial adapters (CH340G, FT232RL, and PL2303HX) on both Windows and Linux operating systems. The result indicate that under the same operating system, the period distribution for different USB to serial adapters appears remarkably similar. Furthermore, the distributions for CH340G, PL2303HX, and FT232RL exhibit narrower ranges and higher accuracy when tested on the Linux system. Under the Windows operating system, the signal period for CH340G was measured to be 100 ± 0.281 ms (MIN=98.57ms, MAX=101.3ms, Range=2.73ms), PL2303HX was 100 ± 0.187 ms (MIN=98.63ms, MAX=101.5ms, Range=2.87ms), and FT232RL was 100 ± 0.271 ms (MIN=98.45ms, MAX=101.5ms, Range=3.05ms). Under the Linux operating system, the signal period for CH340G was measured to be 100 ± 0.074 ms (MIN=99.61ms, MAX=100.3ms, Range=0.69ms), PL2303HX was 100 ± 0.111 ms (MIN=99.43ms, MAX=100.5ms, Range=1.07ms), and FT232RL was 100 ± 0.076 ms (MIN=99.67ms, MAX=100.3ms, Range=0.63ms).

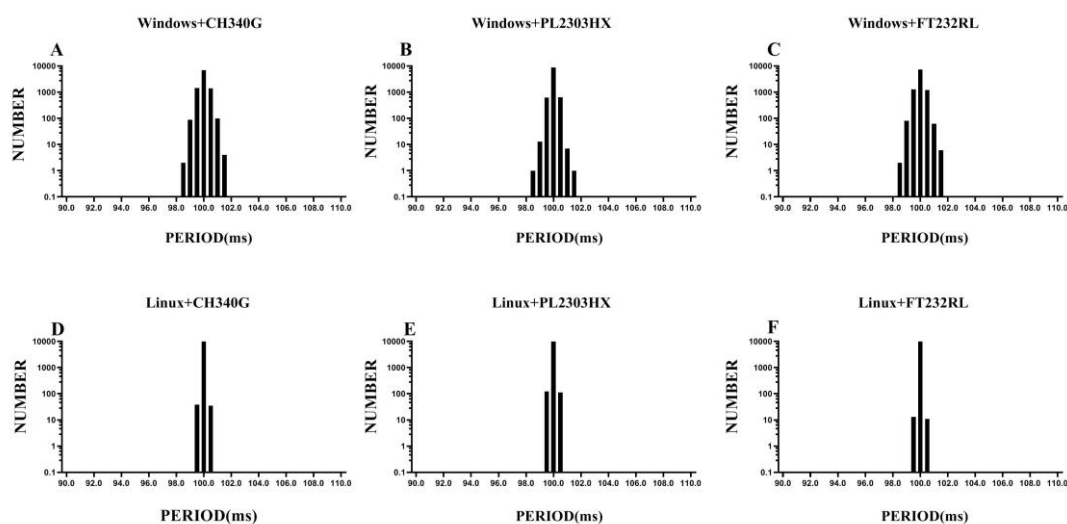


Fig.7 Distributions of Signal Accuracy for Different USB to Serial Adapters and Operating Systems. Notably, under the same operating system, the period distribution for different USB to serial adapters appears remarkably similar. Furthermore, the distributions for CH340G, PL2303HX, and FT232RL exhibit narrower ranges and higher accuracy when tested on the Linux system. These findings suggest that the choice of operating system can significantly impact the precision of USB to serial adapters.

Different API functions have different processing and calling strategies for underlying data, which can also affect the accuracy of serial port synchronization signals. We measured the periodic accuracy of IOPort(), fwrite(), and fprintf() on Windows and Linux. During the test, the USB to serial adapter was CH340G. Figure 8 illustrates the distributions of signal accuracy for different API functions (IOPort(), fwrite(), and fprintf()) on both Windows and Linux operating systems. The result suggest that the choice of API function and operating system can significantly affect the periodic accuracy of serial port synchronization signals. IOPort() shows better accuracy compared to fwrite() and fprintf, and the Linux system generally outperforms the Windows system in terms of signal periodic accuracy. Under the Windows operating system, the signal period for IOPort() was measured to be $100 \pm 0.281\text{ms}$ (MIN=98.57ms, MAX=101.3ms, Range=2.73ms), fwrite() was $100 \pm 0.704\text{ms}$ (MIN=87.77ms, MAX=112.8ms, Range=25.03ms), and fprintf() was $100 \pm 0.795\text{ms}$ (MIN=73.73ms, MAX=127.2ms, Range=53.47ms). Under the Linux operating system, the signal period for IOPort() was measured to be $100 \pm 0.074\text{ms}$ (MIN=99.61ms, MAX=100.3ms, Range=0.69ms), fwrite() was $100 \pm 0.080\text{ms}$ (MIN=99.37ms, MAX=100.6ms, Range=1.23ms), and fprintf() was $100 \pm 0.084\text{ms}$ (MIN=99.37ms, MAX=100.6ms, Range=1.23ms).

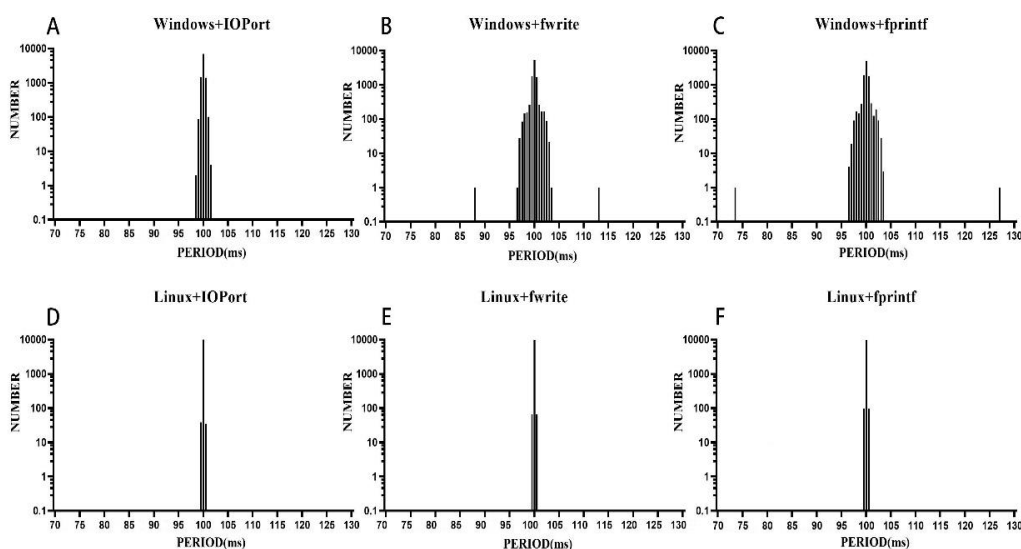


Fig. 8 Distributions of Signal Accuracy for Different API Functions and Operating Systems. Notably, the precision of IOPort() is consistently better than that of fwrite() and fprintf() across both operating systems. Additionally, the Linux operating system generally offers improved precision for the same API function compared to the Windows system. Researchers seeking optimal accuracy in serial port synchronization should consider utilizing the IOPort() function and the Linux operating system to achieve the highest level of precision.

Experiment III

Optical signals can offer a convenient alternative for calculating response latency without time synchronization. However, the discrepancy in position between the optical signal and the visual stimulus can introduce time errors. To address this issue and minimize the error, a high-precision calibration formula has been proposed in this study.

The calibration formula, derived from the VESA standard (Association, 2013), takes into account the timing specifications of the raster scanning mechanism and the time required to light up pixels, lines, and frames on the monitor. Assuming a resolution of $1920 * 1080$ and a refresh rate of 60Hz, the time required to light up one pixel is 6.7ns (t_{PC}), light up one line is $14.8\mu\text{s}$ (t_{HT}), and light up one frame is 16.7ms (t_{VT}). To calculate the accurate visual stimulus presentation time based on the optical signal, the formula utilizes two points, A and B, on the monitor. Point A represents the optical signal with coordinates (X_1, Y_1) , and point B represents the visual stimulus with coordinates (X_2, Y_2) , see Fig.9. The frame interval between points A and B is denoted as n . The high-precision calibration formula, as shown in formula (3), involves the measurement of the moment T_A when the optical signal was presented and the theoretically calculated value T_B representing the moment when the visual stimuli were presented. By applying this calibration formula, researchers can accurately determine the visual stimulus presentation time based on the measured optical signal, thus enabling the precise calculation of response latency.

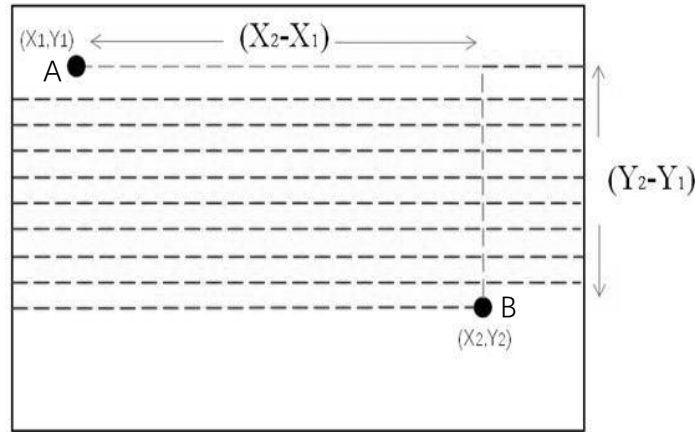


Fig.9 Principle of the Calibration Formula Implementation. Point A represents the location of the optical signal, while point B represents the location of the visual stimulus. By summing the presentation moment of point A and the time required to light up the pixels along the trajectory from point A to point B, we can determine the precise presentation moment of point B.

$$T_B = T_A + (X_2 - X_1) * t_{PC} + (Y_2 - Y_1) * t_{HT} + n * t_{VT} \quad (3)$$

In order to validate the accuracy of the calibration formula, five points on the monitor (computer 1) were selected, as depicted in Fig.10. At each of these points, a black block consisting of one pixel and a

white block consisting of one pixel were alternately displayed with a frequency of 10Hz. To collect the data for validation, a logic analyzer was used to capture two thousand sets of data for each point. The test was conducted with a resolution of 1920 * 1080, a refresh rate of 60Hz, and the monitor preheated for over an hour.

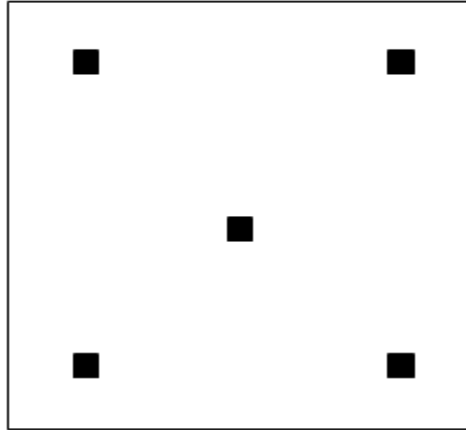


Fig.10 Locations of the Five Selected Points on the Monitor Location of 5 points. The coordinates for each point are as follows: first point: [52, 49, 53, 50], second point: [1871, 50, 1872, 51], third point: [962, 540, 963, 541], fourth point: [52, 1029, 53, 1030], fifth point: [1872, 1029, 1873, 1030].

To assess the accuracy of the calibration formula, two points were selected, one as the optical signal and the other as the visual stimulus. The measurement value of the visual stimulus presentation moment, denoted as T_B' , was obtained, and the error ε of the visual stimulus presentation time was calculated using formula (4). The results, presented in Table 3, show the Mean and SD for each group. For the darkening process, the error ε was found to be $-0.11 \pm 0.10\text{ms}$ (Mean \pm SD), while for the lighting process, the error ε was $-0.73 \pm 0.46\text{ms}$ (Mean \pm SD). Fig.11 displays the error of the calibration formula, with the upper half of the red line corresponding to the darkening process and the lower half corresponding to the lighting process. The graph indicates that the error of the calibration formula during the darkening process is better than that during the lighting process. Therefore, it is recommended to use the darkening process as the optical signal during experimental design, as it yields more accurate results in terms of the calibration formula.

$$\varepsilon = T_B' - T_B = T_B' - [T_A + (X_2 - X_1) * t_{pc} + (Y_2 - Y_1) * t_{HT} + n * t_{VT}] \quad (4)$$

Tab.3 Calibration formula error table (unit: ms). The value format is MEAN \pm SD. Cells are colored pale green where the value is correspond to the darkening process. A dark pink where he value is correspond to the brightening process.

	First Point	Second Point	Third Point	Fourth Point	Fifth Point
First Point		$\varepsilon = -0.01 \pm 0.07$	$\varepsilon = -0.15 \pm 0.06$	$\varepsilon = -0.06 \pm 0.07$	$\varepsilon = -0.23 \pm 0.06$
Second Point	$\varepsilon = 0.03 \pm 0.17$		$\varepsilon = -0.14 \pm 0.06$	$\varepsilon = -0.06 \pm 0.07$	$\varepsilon = -0.23 \pm 0.06$
Third Point	$\varepsilon = -0.72 \pm 0.15$	$\varepsilon = -0.75 \pm 0.16$		$\varepsilon = 0.08 \pm 0.06$	$\varepsilon = -0.09 \pm 0.06$
Fourth Point	$\varepsilon = -1.04 \pm 0.16$	$\varepsilon = -1.07 \pm 0.16$	$\varepsilon = -0.32 \pm 0.14$		$\varepsilon = -0.17 \pm 0.06$
Fifth Point	$\varepsilon = -1.29 \pm 0.15$	$\varepsilon = -1.32 \pm 0.15$	$\varepsilon = -0.57 \pm 0.13$	$\varepsilon = -0.25 \pm 0.13$	

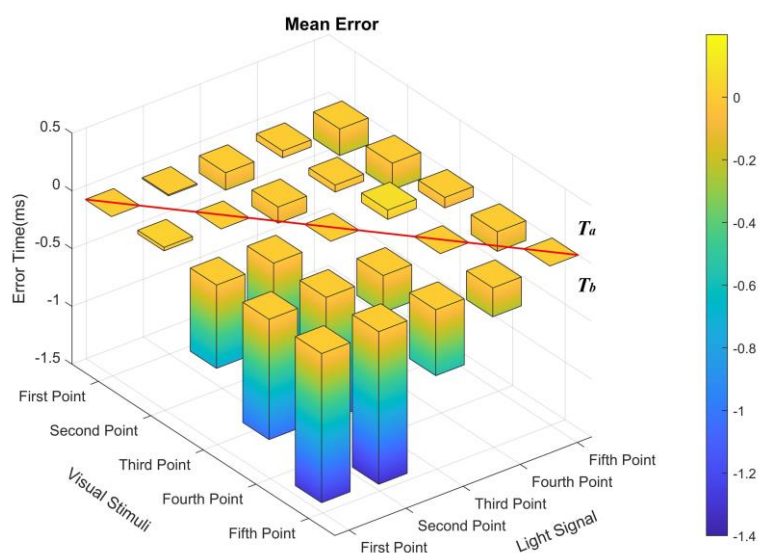


Fig.11 The Mean Error of the Calibration Formula. The graph has a red line, with the upper half representing the darkening process and the lower half representing the brightening process. The blocks corresponding to the red line indicate scenarios where the optical signal and visual stimulation were at the same point, resulting in a time error of 0.

Discussion

Response latency plays a crucial role in elucidating the intricate mechanisms involved in encoding and transmitting information within the nervous system (MAUNSELL et al., 1999). To ensure accurate measurement of response latency, it is imperative that all devices involved maintain synchronized time. In the experimental design, visual stimuli were presented prior to the serial port synchronization signals. However, contrary to this design, the most noteworthy finding is that $T_a < 0$ and $T_b < 0$, indicating that the serial port synchronization signals precede the visual stimuli. These findings have shed new light on the

timing dynamics and synchronization between visual stimuli and serial port signals. This discovery highlights the need for a comprehensive investigation into the underlying factors contributing to this lead and emphasizes the importance of optimizing the accuracy of response latency measurements in future research endeavors.

This phenomenon can be attributed to the inherent complexity of the visual stimulus presentation process compared to the relatively simpler serial port signals. The general loop of stimulus presentation is that: 1) Sending the drawing commands to the graphics card (GPU), such as Screen('Flip'). 2) The GPU processes these commands to generate the image to be displayed next. 3) Rendered the new image into an invisible back buffer. 4) Swapped the back and front buffer. 5) Reading out and displays the content of the front buffer (Kleiner, Brainard, & Pelli, 2007; Poth, et al., 2018). Considering Figure 3A as an example, according to the VESA standard, the time required for the monitor to light up the pixel at line 141 and column 92 is 1.97ms (based on a resolution of 1920 * 1080 and a refresh rate of 60Hz). Additionally, the response time of the LCD monitor is 1ms. Thus, the total time required for the monitor to light up this pixel is at least 2.97ms. The result from He Feng suggested that the serial port delay during power transmission may be less than 2ms (Feng et al., 2009). While this observation alleviates concerns regarding excessive lag, it also presents new challenges. For instance, in the conventional experimental setup where the visual stimulus is centered on the display and the refresh rate is 60Hz, the serial port synchronization signal may be approximately 10ms ahead of the visual stimulus (as illustrated in Figures 5C and 5D), which is considered unacceptable. In light of this, researchers must carefully consider the specific characteristics of their experimental setup and measure the timing and time error of their system accordingly.

We have observed several important factors influencing the lead time and accuracy of the serial port synchronization signal. Firstly, the lead time is affected by the refresh rate and the position of the visual stimuli. A higher refresh rate leads to shorter lead times, while deviations of the stimulus position towards the right and downwards result in longer lead times. Thus, if minimizing time errors is crucial, it is advisable to position the stimulus in the upper left corner and set the highest available refresh rate. Secondly, the accuracy of the serial port synchronization signal is influenced by the operating system and the API. Under Linux, using the IOPort() yields better accuracy compared to other operating systems. This discrepancy may stem from the fact that Linux accesses hardware through file-based interactions, eliminating the need for

device drivers and potentially enhancing accuracy (Jun-ling & Peng-fei, 2005; Xiao-cheng, Jia-hua, & Feng, 2010). Additionally, the choice of API plays a role, as `fprintf()` is typically used for writing ASCII values to files, while `fwrite()` handles binary data (Schildt, 2003). In contrast, `IOport()` is specifically designed for precise control of input/output hardware, leading to superior serial signal accuracy. By considering these factors and making appropriate adjustments in experimental design, researchers can minimize time errors and optimize the accuracy of their response latency measurements.

Given the complexities and potential sources of error in the serial port synchronization signal, we suggest utilizing optical signals as an alternative method for measuring response latency. Optical signals offer a more direct and convenient approach, without the need for time synchronization between devices. To address the time error between the optical signal and visual stimuli, we have proposed a high-precision calibration formula. Our findings indicate that when using the darkening process as the optical signal, the time error is less than 0.5ms, demonstrating significantly better performance compared to the brightening process. This improvement may be attributed to the monitor's faster response during the grayscale reduction process (H & A, 2007; T & G, 2009; Zhang et al., 2018).

In experimental settings, we recommend employing the darkening process as the optical signal and utilizing the calibration formula to accurately calculate the presentation time of visual stimuli. By implementing this approach, researchers can obtain precise response latency measurements. Overall, the use of optical signals combined with the proposed calibration formula offers a promising solution to enhance the accuracy of response latency measurements in experimental studies.

Conclusion

The serial port synchronization signal has been widely used for time synchronization in research experiments. It is crucial for researchers to measure the accuracy of the serial port synchronization signal and its timing with visual stimuli before conducting experiments. Additionally, efforts should be made to optimize the synchronization process in subsequent experiments. In comparison to the serial port signal, optical signals offer a more direct and intuitive approach for synchronization as they closely follow the same principles as visual stimuli. Furthermore, optical signals eliminate the need for clock synchronization between devices. By utilizing the calibration formulas developed in this study, researchers can achieve an error less than 0.5ms in determining the moment of visual stimulus presentation using optical signals,

particularly when employing the darkening process. It is strongly recommended to adopt this method. The findings of this study provide valuable insights for optimizing experimental design and improving the accuracy of response latency measurements.

Acknowledgments

The authors gratefully acknowledge support from the Social Science Foundation of Anhui Province of China (Grant Number: AHSKF2019D014) .

Declarations

Funding The study funding provided by the Social Science Foundation of Anhui Province of China under Grant (No. AHSKF2019D014).

Competing Interests The authors declare no competing interests.

Ethics Approval Not applicable.

Consent to Participate Not applicable.

Consent for Publication Not applicable.

Data Availability The dataset used for the example run described here can be downloaded from <https://github.com/chenxu2656/The-Discrepancy-In-Timing>

Code Availability The whole code can be downloaded from <https://github.com/chenxu2656/The-Discrepancy-In-Timing>

Open Practices Statements Data and code are made freely available for other colleagues.

References

- Arieh, Y., & Marks, L. E. (2008). Cross-modal interaction between vision and hearing: a speed-accuracy analysis. *Percept Psychophys*, 70(3), 412-421. Retrieved from <https://www.ncbi.nlm.nih.gov/pubmed/18459251>. doi:10.3758/pp.70.3.412
- Association, V. E. S. (2013). VESA and Industry Standards and Guidelines for Computer Display Monitor Timing.pdf. In (pp. 1-105): Video Electronics Standards Association
- Bridges, D., Pitiot, A., R, M., MacAskill, & W.Peirce, J. (2020). The timing mega-study comparing a range of experiment generators both lab-based and online.pdf. *PeerJ*, e9414. doi:10.7717/peerj.9414

- Eileen L. Troconis, Alexander J. Ordoobadi, Thomas F. Sommers, Razina Aziz-Bose, Ashley R. Carter, & Trapani, J. G. (2016). Intensity-dependent timing and precision of startle response latency in larval zebrafish.pdf. *The Journal of Physiology*, 1-18. doi:10.1113/JP272466
- Feng, H., Yong, Z., YaBo, L., & Rui, G. (2009). Measurement and analysis of the timing delay for serial port in PC. *Science of Surveying and Mapping*, 34, 41-43.
- Gao, Z., Chen, B., Sun, T., Chen, H., Wang, K., Xuan, P., & Liang, Z. (2020). Implementation of stimuli with millisecond timing accuracy in online experiments.pdf. *PloS one*, 15, e235249. doi:10.1371/journal.pone.0235249
- H, L., & A, B. (2007). Temporal response of medical liquid crystal displays.pdf. *MedPhys*, 34, 639-646. doi:10.1118/1.2428403 兴
- Jun-ling, L., & Peng-fei, W. (2005). The Implementation and Cmparision of Serial Communication in Linux and Windows.pdf. *Journal of YuLin College*, 12-14.
- Kleiner, M., Brainard, D., & Pelli, D. (2007). What's new in Psychtoolbox-3?.pdf. *PERCEPTION*, 36S, 14.
- Levakova, M., Tamborrino, M., Ditlevsen, S., & Lansky, P. (2015). A review of the methods for neuronal response latency estimation. *Biosystems*, 136, 23-34. Retrieved from <https://www.ncbi.nlm.nih.gov/pubmed/25939679>. doi:10.1016/j.biosystems.2015.04.008
- MAUNSELL, J. H. R., GHOSE, G. M., ASSAD, J. A., MCADAMS, C. J., BOUDREAU, C. E., & NOERAGER, B. D. (1999). Visual response latencies of magnocellular and parvocellular LGN neurons in macaque monkeys.pdf. *Visual Neuroscience*, 16, 1-14.
- Nguyen, K. T., Liang, W.-K., Muggleton, N. G., Huang, N. E., & Juan, C.-H. (2019). Human visual steady-state responses to amplitude-modulated flicker : Latency measurement.pdf. *Journal of Vision*, 19, 1-17. doi:10.1167/19.14.14
- Poth, , C. H., Foerster, , R. M., Behler, , C., Schwanecke, , U., Schneider, , W. X., & Botsch, M. (2018). Ultrahigh temporal resolution of visual presentation using gaming monitors and G-Sync.pdf. *Behavior Research Methods*. doi:10.3758/s13428-017-1003-6
- Schildt, H. (2003). *C++: The Complete Reference.pdf* (Fourth ed.): McGraw-Hill Osborne Media.
- T, E. (2010). Achieving precise display timing in visual neuroscience experiments..pdf. *J Neurosci Methods*, 191, 171-179. doi:10.1016/j.jneumeth.2010.06.018
- T, E., & G, T. T. (2009). Liquid crystal display response time estimation for medical applications.pdf. *Med Phys*, 36, 4984-4990. doi:10.1118/1.3238154 兴
- T, E., & L, G. P. (2010). Misspecifications of stimulus presentation durations in experimental psychology A systematic review of the psychophysics literature .pdf. *PloS one*, 5, e9414. doi:10.1371/journal.pone.001279210.1371/journal.pone.0012792.g001
- Xiangrui, L., Liang, Z., Kleiner, M., & Zhong-Lin, L. (2010). RTbox A device for highly accurate response time measurements.pdf. *Behavior Research Methods*, 42, 212-225. doi:10.3758/BRM.42.1.212
- Xiao-cheng, L., Jia-hua, Z., & Feng, L. (2010). Application of Serial Communication in Industrial Control Based on Linux.pdf. *Machine Building & Automation*, 39(96-98).
- Yap, M. J., Balota, D. A., Cortese, M. J., & Watson, J. M. (2006). Single- versus dual-process models of lexical decision performance: insights from response time distributional analysis. *J Exp Psychol Hum Percept Perform*, 32(6), 1324-1344. Retrieved from <https://www.ncbi.nlm.nih.gov/pubmed/17154775>. doi:10.1037/0096-1523.32.6.1324

-
- Zamarashkina, P., Popovkina, D. V., & Pasupathy, A. (2020). Timing of response onset and offset in macaque V4: stimulus and task dependence.pdf. *Journal of Neurophysiology*, *123*, 2311-2325. doi:10.1152/jn.00586.2019
- Zhang, G.-L., Li, A.-S., Miao, C.-G., He, X., Zhang, M., & Zhang, Y. (2018). A consumer-grade LCD monitor for precise visual stimulation.pdf. *Behavior Research Methods*, *50*, 1496-1502. doi:10.3758/s13428-018-1018-7